Improved Velocity Estimation Using Single Loop Detectors

Benjamin Coifman, PhD

Assistant Professor, Civil and Environmental Engineering and Geodetic Science
Assistant Professor, Electrical Engineering

Ohio State University
470 Hitchcock Hall
2070 Neil Ave
Columbus, OH 43210-1275

Coifman.1@OSU.edu
http://www-ceg.eng.ohio-state.edu/~coifman
614 292-4282

Submitted for publication in Transportation Research-B

ABSTRACT

This paper develops an improved algorithm for estimating velocity from single loop detector data. Unlike preceding works, the algorithm is simple enough that it can be implemented using existing controller hardware. The discussion shows how the benefits of this work extend to automated tests of detector data quality at dual loop speed traps. Finally, this paper refutes an earlier study that found conventional single loop velocity estimates are biased.

Keywords:
traffic surveillance, loop detectors, velocity estimation, data screening

INTRODUCTION

Loop detectors are the preeminent vehicle detector for freeway traffic surveillance. They are frequently deployed as single detectors, i.e., one loop per lane per detector station. Although single loops have been used for decades, debate continues on how to interpret the measurements and how to calibrate the detectors. In conventional practice, the single loop measurements are very noisy and many researchers have sought sophisticated filtering methods, e.g., Mikhalkin et al (1972), Pushkar et al (1994), and Dailey (1999). Unfortunately, most of the preceding efforts focused on complicated models without explicitly identifying the sources of error. The earlier works also lose sight of the end goal: to produce an algorithm that can be deployed on a simple processor, such as a Model 170 controller.

This paper provides a new perspective by clarifying the source of several errors and suggesting ways to reduce the impacts. The body of this work emphasizes velocity estimation, but it has implications for tests of detector data quality as well. The first section reviews the state of the practice for parameter measurement and estimation from single loop detectors. The next section illustrates how conventional practice may be susceptible to changes in the vehicle population throughout the day as well as errors due to sample size. The paper continues by developing an algorithm to overcome these problems. Finally, the discussion shows how the work has implications for tests of detector data quality and elucidates the findings of an earlier study that concluded that single loop velocity estimates are biased.

PARAMETER MEASUREMENT AND ESTIMATION

Conventional single loop detectors are capable of measuring flow, the number of vehicles that pass the detector during a fixed sample period, and occupancy, the percentage of the given sample period that the detector is "occupied" by vehicles. For each lane, these two parameters are defined as:

$$q_k = \frac{n_k}{T} \tag{1A}$$

$$\theta_k = \frac{\sum_{j \in J_k} t_j}{T} \tag{1B}$$

where the subscript "k" indicates the given sample, subscript "j" indicates vehicle specific parameters and

q_k = flow during sample k

θ_k = occupancy during sample k

n_k = number of vehicles that pass the detector during sample k

T = sampling period

J_k = set of all vehicles that pass the detector during sample k

t_j = vehicle j's *on time*.

Two interdependent vehicle parameters are of interest for estimating mean sample velocity: vehicle velocity and vehicle length. The relationship between these two parameters for a vehicle passing over a loop detector is simply:

$$L_j = L_j^v + L_j^s = v_j \cdot t_j \tag{2}$$

where

L_j = vehicle j's effective length as "seen" by the detector

L_j^v = vehicle j's true length

L_j^s = length of detector's sensitivity region for vehicle j

v_j = vehicle j's velocity

The length of the detector's sensitivity region typically depends on many variables such as the vehicle's position in the lane, height of the vehicle's underframe, and the amount of ferrous metal in the vehicle. It is difficult to separate this length from the vehicle's true length using loop detector data, so for the rest of this paper "length" will refer to the sum of these two lengths, often referred to as the effective vehicle length.

From equations 1 and 2,

$$\theta_k = \frac{1}{T}\sum_{j \in J_k}\frac{L_j}{v_j} = q_k \cdot \frac{1}{n_k}\sum_{j \in J_k}\frac{L_j}{v_j} \tag{3A}$$

assuming that individual vehicle lengths and velocities are uncorrelated,

$$\theta_k \approx \frac{q_k \cdot \overline{L}_k}{\overline{v}_k} \tag{3B}$$

where

$\overline{L}_k$ = arithmetic mean vehicle length for sample k

$\overline{v}_k$ = harmonic mean vehicle velocity for sample k, often referred to as the *space mean speed*.

In other words,

$$\overline{v}_k \approx \frac{q_k \cdot \overline{L}_k}{\theta_k} \tag{4}$$

Equation 4 shows the relationship between mean velocity and mean length, but these two parameters can not be measured independently at a single loop. Typically, an operating agency will use one of two approaches to address this problem. In the first case, $\overline{L}_k$ is simply set to a constant value, $\hat{L}$, and Equation 5 is used to estimate $\overline{v}_k$:

$$\hat{v}_k = \frac{q_k \cdot \hat{L}}{\theta_k} \tag{5}$$

There are many site specific variables that can influence the mean vehicle length, such as the percentage of long vehicles in the lane and the detector's sensitivity. So, other operating agencies assume a fixed free flow velocity and reversing the assignment in Equation 5, estimate $\hat{L}$ each day during periods when traffic over the detector is almost certain to be free flowing. Then, $\hat{L}$ is held fixed during the remainder of the day and the velocity estimation progresses using Equation 5 directly.

ANALYSIS

Some of the site specific variables are corrected with a daily estimate of $\hat{L}$, but other factors are not addressed, such as the possibility that the percentage of long vehicles may change during the day or the simple fact that a sample with few vehicles (i.e., low flow) may not have a representative sample of vehicle lengths. For this study, we examine 24 hours of detector actuations, sampled at 60 Hz, for each lane at a detector station on Interstate-80 in Berkeley, California. The data come from dual loop *speed traps*, where a speed trap consists of two closely spaced loop detectors in the same lane. In this configuration, it is possible to measure true vehicle velocities by dividing the loop separation by the difference in arrival times at each loop. Finally, $\overline{L}_k$ is calculated using Equation 4 by assuming absolute equality.

Figure 1A illustrates the time series evolution of $\overline{L}_k$ for the eastbound traffic with $T = 15\,\text{min}$. Following Caltrans convention, lanes are numbered starting at the inside and increasing outward. The legend indicates the total number of vehicles in each lane during the day. Including the westbound data (not shown), the observed values of $\overline{L}_k$ range from 19 feet to 51 feet and almost all lanes exhibit a strong temporal dependency. Figure 1B-C show the corresponding n_k and $\overline{v}_k$, respectively.

When an operating agency estimates $\hat{L}$, they typically sample the value during early morning hours. As one would expect, these hours are free flowing for this example; however, they also correspond to the highest values of $\overline{L}_k$ and lowest values of q_k. Thus, if $\hat{L}$ were estimated strictly during the early morning, estimates of velocity from Equation 5 would be too high throughout the remainder of the day. Since the phenomena depend on site specific factors, the figures indicate the need for an improved method of estimating $\hat{L}$ on-line.

Figure 2 shows the cumulative distribution of $\overline{L}_k$ for the eastbound lanes using four different sampling periods. Although Lane 1 shows little variance due to a truck restriction, the other lanes exhibit a large variance. So no single value of $\hat{L}$ will be representative of all samples and a value of $\hat{L}$ estimated using one value of T might not be valid for another value of T.

The primary source of this variance comes from the fact that the vehicles observed during a given sample may not be "typical". Figure 3 shows the observed distribution of individual vehicle lengths for the eastbound traffic. Approximately 85 percent of the vehicles are between 15 and 22 feet, but some are as long as 80 feet or roughly four times the median length. When n_k is small, i.e., low flow, a long vehicle can skew θ_k simply because it takes more time for the long vehicle to pass the detector.

In accordance with the law of large numbers, the sample distribution should become more representative of the entire population as n_k increases, which in turn, increases with q_k and T. Figure 4 illustrates this phenomena using the eastbound data from all lanes for three values of T. The top half of the figure shows $\overline{L}_k$ during free flow conditions, $\overline{v}_k$ > 50 mph, while the lower half shows $\overline{L}_k$ during congestion, $\overline{v}_k$ < 50 mph. In parts A and D, where $T = 30\,\text{sec}$, the maximum number of vehicles per sample is so small that the observations fall into distinct columns, i.e., the first column contains observations with only one vehicle, the second column contains observations with only two vehicles, and so on. Notice that for each T, the range of $\overline{L}_k$

decreases as q_k increases; also note that in this data set, the lowest flows are only observed during free flow conditions.

Improving the Length Estimates

As previously noted, a single loop detector can not measure $\bar{v}_k$ directly and estimates of $\hat{L}$ may be biased by the time of day. To overcome these problems, $\hat{L}$ is estimated during periods when the traffic should be free flowing. Rather than choosing a period of the day a priori, the data are used to make the distinction. Empirically, free flow conditions correspond to low occupancies and Equation 3B explicitly shows that θ_k is inversely proportional to $\bar{v}_k$. For this study, a sample is considered free flowing if

$$\theta_k < \theta_{threshold} \tag{6}$$

where $\theta_{threshold}$ was set to 10 percent. The value was chosen so that most free flow samples would be selected, but low enough to ensure that very few (if any) congested samples are selected. In practice, this threshold could be set from a plot of flow versus occupancy. To account for samples with high θ_k due to free flowing trucks, for $T = 30\,\text{sec}$, a sample is also considered free flowing if at least half of the 10 preceding samples satisfy Equation 6. Next,

$$\hat{L} = v_{ff} \cdot mean\left(\frac{\theta_k}{q_k}\right) \forall k \in K \tag{7}$$

where

v_{ff} = assumed fixed free flow velocity, set to 60 mph for this study

K = set of all free flow samples with $q_k > 0$ and $\theta_k > 0$ in the given lane during the 24 hour study.

The resulting $\hat{L}$ for the eastbound traffic are shown in Table 1. Using these values and Equation 5 to calculate $\hat{v}_k$, Figure 5 shows $\hat{v}_k$ versus $\bar{v}_k$ over entire 24 hour study. The solid line in each plot indicates where the estimated values equal the measured values. Note that $\hat{v}_k$ ranges between 20 mph and 120 mph for samples with $\bar{v}_k$ > 50 mph. In other words, the estimate is very noisy when the traffic is free flowing. The noise is primarily due to the variance in $\bar{L}_k$ at low flow (recall from Equations 4-5, $\hat{v}_k \approx \bar{v}_k \cdot \hat{L}/\bar{L}_k$). Finally, consider the congested observations, $\bar{v}_k$ < 50 mph. In each lane the observations are roughly collinear and the guess of v_{ff} serves as a scaling factor, increasing or decreasing the slope of the congested data. In lane 1, the guess of v_{ff} was too low and the estimated velocities are lower than the measured velocities, while in lanes 3 and 4, the opposite is true. This error is included in the plots because it can not be eliminated from single loop detector data without additional detectors.

The analysis is repeated with $T = 5\,\text{min}$ to reduce the estimate noise. Now, however, a sample is only considered free flowing if it satisfies Equation 6 or the preceding sample satisfied Equation 6. Once more the resulting $\hat{L}$ are shown in Table 1, while Figure 6 shows $\hat{v}_k$ versus $\bar{v}_k$ for $T = 5\,\text{min}$. Even with the longer sampling period, the estimates are still noisy when the traffic is free flowing.

To illustrate the effects of different values of v_{ff} or $\hat{L}$, consider the percent error in $\hat{v}_k$ relative to $\bar{v}_k$ over the entire day for various fixed values of $\hat{L}$. Figure 7 shows contour plots of the percent error as $\hat{L}$ ranges between 16 and 32 feet for two different lanes when $T = 30\,\text{sec}$ and $T = 5\,\text{min}$. For example, when $\hat{L}$ = 19 feet in Figure 7A, approximately 70 percent of the estimated velocities are within 5 percent of the measured values. Comparing the top plot to the bottom plot in either lane, the longer sampling period increases n_k and thus, reduces the error. Notice that the optimal value of $\hat{L}$ appears to depend on T in the right-hand plots (lane 5 westbound), reaffirming the fact that $\hat{L}$ estimated at one value of T may not be valid for another value of T. The figure also shows that performance is relatively stable for length estimates within a few feet of the optimal value.

Improving the Velocity Estimates

Free flow velocity estimates are poor during low flow, but from an operational standpoint, it is sufficient to know that traffic is free flowing during these conditions. This supposition is implicit with on-line estimation of $\hat{L}$. Once more, exploiting the fact that free flow, low flow samples are characterized by low occupancy, the estimated velocity can be set to a constant value, $\hat{v}_k = v_{ff}$ when $\theta_k < \theta_{threshold}$. Rewriting Equation 5 to include this constraint:

$$\hat{v}_k = \begin{cases} \dfrac{q_k \cdot \hat{L}}{\theta_k}, & \theta_k \geq \theta_{threshold} \\ v_{ff}, & \theta_k < \theta_{threshold} \end{cases} \tag{8}$$

To illustrate the benefits of this constraint, return to the data in Figure 6. Recalculating $\hat{v}_k$ using Equation 8 with $\theta_{threshold} = 10\%$, the new relationships are shown in Figure 8. Notice that almost all of the noise has been eliminated from the estimates corresponding to samples with $\bar{v}_k$ > 50 mph. Figure 9 compares the time series $\hat{v}_k$ from Equation 5, $\hat{v}_k$ from Equation 8, and $\bar{v}_k$. In this figure, one can see that Equation 8 removed many erroneous velocity estimates, particularly during the early morning. Applying Equation 8 to the 30 second data yields similar results, as shown in Figure 10.

IMPLEMENTATION

The analysis for $T = 30\,\text{sec}$ used a moving average to identify free flow periods with high θ_k, but a moving average is memory intensive. In contrast, exponential filtering can accomplish the same goal with almost no data storage. The following pseudo-code can be used to implement the method presented above:

if $\theta_k > 0$ and $q_k > 0$

  if $\theta_k < 10\%$ or $u > 0.1$

    $$\hat{L} = v_{ff} \cdot mean\left(\frac{\theta_k}{q_k}\right) \cdot r + \hat{L} \cdot (1 - r)$$

    $$\hat{v}_k = v_{ff}$$

    $$u = 1 \cdot p + u \cdot (1 - p)$$

  else

    $$\hat{v}_k = \frac{q_k \cdot \hat{L}}{\theta_k}$$

    $$u = 0 \cdot p + u \cdot (1 - p)$$

  end

end

where

r = filtering factor with a time constant on the order of a week (to minimize the time of day dependency illustrated in Figure 1A), e.g., $r = 1/20000$ for $T = 30\,\text{sec}$ and $r = 1/2000$ for $T = 5\,\text{min}$.

p = filtering factor with a time constant on the order of 5 minutes, e.g., $p = 0.2$ for $T = 30\,\text{sec}$ and $p = 1$ for $T = 5\,\text{min}$.

u = an indicator variable used in conjunction with p to determine whether preceding samples were free flowing.

Rather than using a static assignment of $\hat{L}$, as in Equation 7, the algorithm uses an exponential filter to dynamically update $\hat{L}$. This pseudo-code is presented to show that the method can be implemented easily, but it is left to future research to determine the optimal implementation.

DISCUSSION

Implications Beyond Single Loop Velocity Estimates

The impact of this work to single loop detectors is straightforward, but this work has implications for dual loop speed traps as well. Earlier studies have developed automated tests of detector data quality, e.g., Jacobson et al (1990), Cleghorn et al (1991), and Nihan (1997). Their goal is to eliminate erroneous measurements due to transient problems or component failures. Similar systems often go undocumented in the literature because they are either designed in-house by an operating agency or a consulting firm (see Chen and May, 1987, for examples). Most of these data quality tests can be expressed using the following constraint to bound *good* speed trap data:

$$\bar{v}_k \in \left[\frac{q_k \cdot L_{\min}(q_k, \bar{v}_k, \theta_k)}{\theta_k}, \frac{q_k \cdot L_{\max}(q_k, \bar{v}_k, \theta_k)}{\theta_k} \right] \tag{9A}$$

where $L_{\min}$ and $L_{\max}$ are lower and upper bounds, respectively, that may depend on q_k, $\bar{v}_k$ or θ_k. Naturally, this constraint reduces to the following for single loop detector data:

$$\hat{v}_k \in \left[\frac{q_k \cdot L_{\min}(q_k, \theta_k)}{\theta_k}, \frac{q_k \cdot L_{\max}(q_k, \theta_k)}{\theta_k} \right] \tag{9B}$$

Some of these tests fail to accommodate the fact that the variance in $\bar{L}_k$ increases as q_k decreases. The author recently identified such a system currently in use by a large operating agency. In particular, the agency applied Equation 9A, using fixed values of $L_{\min}$ and $L_{\max}$, to speed trap data.

The test discarded almost all early morning observations from the agency's 400 detector stations simply because the constraint is too restrictive during low occupancy conditions.

Previous Research in the Context of the new Analysis

There has been some confusion in the discipline since Hall and Persaud (1989) concluded that, for a fixed value of $\hat{L}$, Equation 5 does not hold over an extended range of occupancies. Their paper examined the "g-factor" which is simply the inverse of $\hat{L}$, and the analysis used,

$$g = \frac{1}{\overline{L}_k} \tag{9}$$

Roughly summarizing their plots of g versus occupancy: g decreases by a factor of two from one percent to five percent occupancy, remains constant over the range of five percent to 40 percent occupancy, and then drops by an order of magnitude from 40 percent to 80 percent occupancy. To reduce errors due to vehicle lengths, they selected lanes with truck restrictions. In an attempt to reproduce these results, Figure 11A shows the g-factor versus occupancy for lane 1 eastbound. The g-factor does not exhibit the predicted occupancy dependence. There is one difference, however, the earlier study used occupancy expressed in integer percent. After truncating percent occupancy to integer values and recalculating g, Figure 11B shows the new g-factor versus integer percent occupancy. This plot exhibits the non-linearity at low occupancies predicted by Hall and Persaud, but it does not show the drop in g at high occupancy. Finally, using *time mean speed*[1] rather than *space mean speed* and the truncated occupancy to calculate g, Figure 11C follows the predictions from the earlier study. Figure 12 compares the various methods of calculating the g-factor. It shows mean g-factor over one percent ranges up to 35 percent occupancy and then over five percent ranges through 50 percent occupancy. Note that by using *time mean speed* without truncating occupancy, the g-factor follows the predictions for high occupancy but it does not follow the predictions for low occupancy.

These figures clearly show that subtle differences in aggregation can lead to significant differences in parameter relationships. The tools and data necessary for this detailed analysis were not available to researchers when Hall and Persaud published their work. Although their diagnosis seems to be incorrect, Hall and Persaud correctly identified a significant problem with conventional velocity estimation. An operating agency should expect to encounter similar round-off errors at

---

[1] The arithmetic mean of each samples' vehicle velocities.

low occupancy if they use truncated occupancy to estimate $\hat{L}$ and this error will propagate to all subsequent velocity estimates. In the course of their analysis, Hall and Persaud assumed the operating agency was measuring *space mean speed* when in fact it appears that the agency was measuring *time mean speed*. This measurement error would explain their results at high occupancy. To prevent such oversights in the future, researchers should learn the subtle details of the data measurement and aggregation procedures underlying their detector data. One must remember that loop detectors, as well as most other vehicle detectors, are not precision instruments. To keep the detectors affordable, they are typically designed to meet existing operational needs with minimal excess performance. Finally, recall that the results in Figure 12 represent a lane with a truck restriction. As shown earlier in this paper, when trucks are present, the large range of possible vehicle lengths will reduce the accuracy of velocity estimates from single loops.

CONCLUSIONS

The significance of this work to single loop detectors is straightforward. Figure 7 shows that no single estimate of $\hat{L}$ is appropriate for all samples; but fortunately, for most samples, it is sufficient for the estimate to be within a few feet of the optimal value. Significant errors occur at low flows, however, since the variance in $\bar{L}_k$ increases as q_k decreases. This variance degrades the velocity estimation because $\bar{L}_k$ is less likely to be *average*, as shown in Figure 4. Exploiting the fact that the low flow free flow samples are characterized by low occupancy, the paper has shown that it is possible to identify these conditions and simply report that traffic is *free flowing* (Figures 9-10). This paper has presented improved methods for estimating $\hat{L}$ and $\hat{v}_k$ incorporating these findings. Unlike many preceding works, the approach is simple enough that it can be implemented on existing traffic controllers that have limited processing power, such as a Model 170 controller. Although the implementation is fairly simple, this work has wide ranging implications for practitioners and researchers. For example, the discussion shows how the work is applicable to automated tests of detector data quality, both from dual and single loop detectors. Then, the paper closes by refuting an earlier study, showing that in the presence of a truck restriction, the use of a single estimate $\hat{L}$ in Equation 5 is indeed valid over an extended range of occupancies provided care is taken to measure the right parameters and prevent round-off errors.

REFERENCES

Chen, L., and May, A. (1987) Traffic Detector Errors and Diagnostics. *Transportation Research Record 1132*, pp 82-93. Transportation Research Board, Washington, DC.

Cleghorn, D., Hall, F., and Garbuio, D. (1991) Improved Data Screening Techniques for Freeway Traffic Management Systems. *Transportation Research Record 1320,* pp 17-31. Transportation Research Board, Washington, DC.

Dailey, D. (1999) A Statistical Algorithm for Estimating Speed from Single Loop Volume and Occupancy Measurements. *Transportation Research-B,* Vol 33B, No 5, June 1999, pp 313-322.

Hall, F., Persaud, B. (1989) Evaluation of Speed Estimates Made with Single-Detector Data from Freeway Traffic Management Systems. *Transportation Research Record 1232*, pp 9-16. Transportation Research Board, Washington, DC.

Jacobson, L, Nihan, N., and Bender, J. (1990) Detecting Erroneous Loop Detector Data in a Freeway Traffic Management System. *Transportation Research Record 1287*, pp 151-166. Transportation Research Board, Washington, DC.

Mikhalkin, B., Payne, H., Isaksen, L. (1972) Estimation of Speed from Presence Detectors. *Highway Research Record 388,* pp 73-83. Highway Research Board, Washington, DC.

Nihan, N. (1997) Aid to Determining Freeway Metering Rates and Detecting Loop Errors. *Journal of Transportation Engineering*, Vol 123, No 6, November/December 1997, pp 454-458.

Pushkar, A., Hall, F., Acha-Daza, J. (1994) Estimation of Speeds from Single-Loop Freeway Flow and Occupancy Data Using Cusp Catastrophe Theory Model. *Transportation Research Record 1457*, pp 149-157. Transportation Research Board, Washington, DC.

Figure 1, (A) True $\bar{L}_k$ by lane as a function of time for the eastbound lanes on a single day, T = 15 minutes, and the corresponding (B) number of vehicles per sample (C) measured velocities.

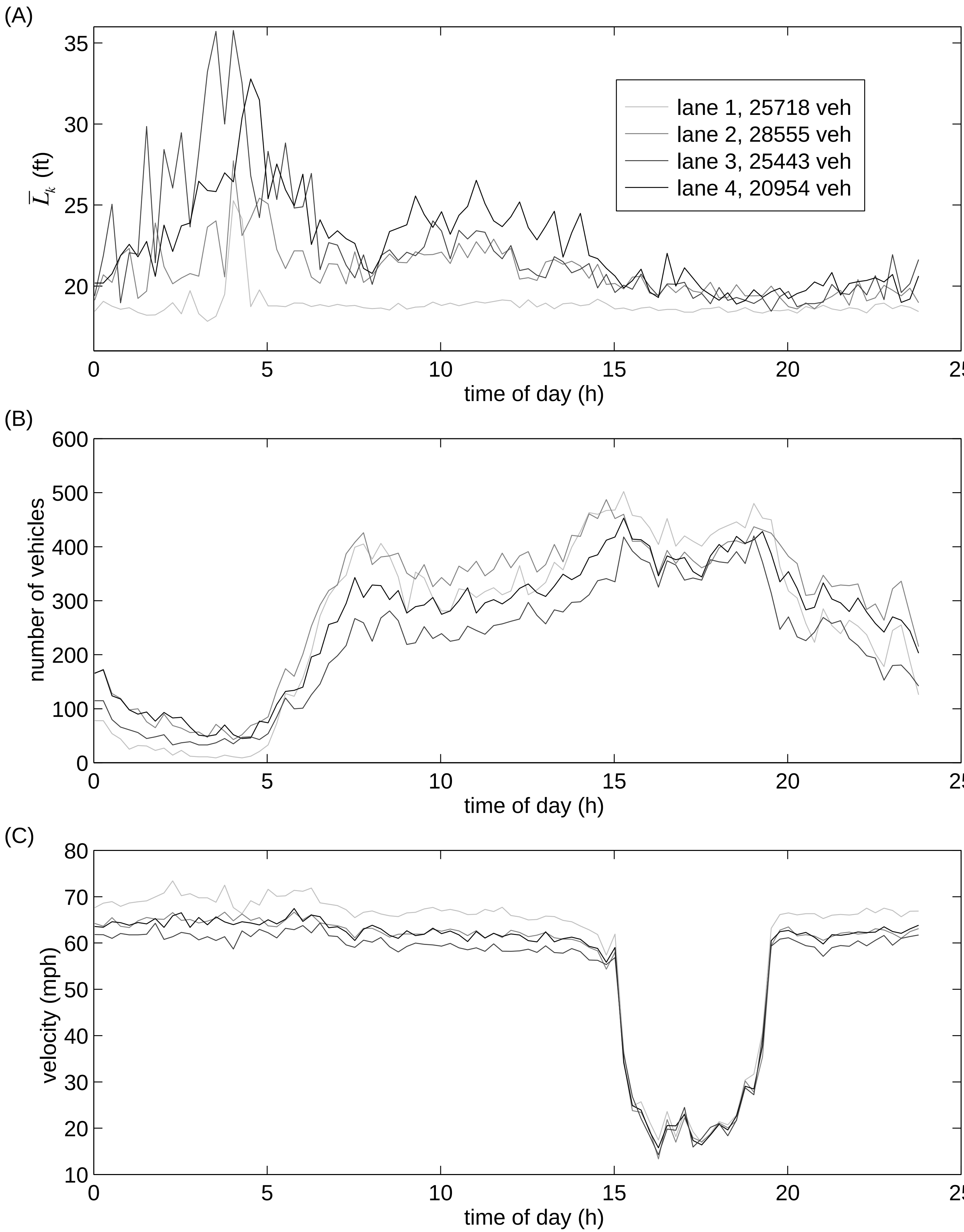

Figure 2, Cumulative distribution of the true $\overline{L}_k$ over 24 hours for the eastbound traffic, (A) lane 1 (B) lane 2 (C) lane 3 (D) lane 4.

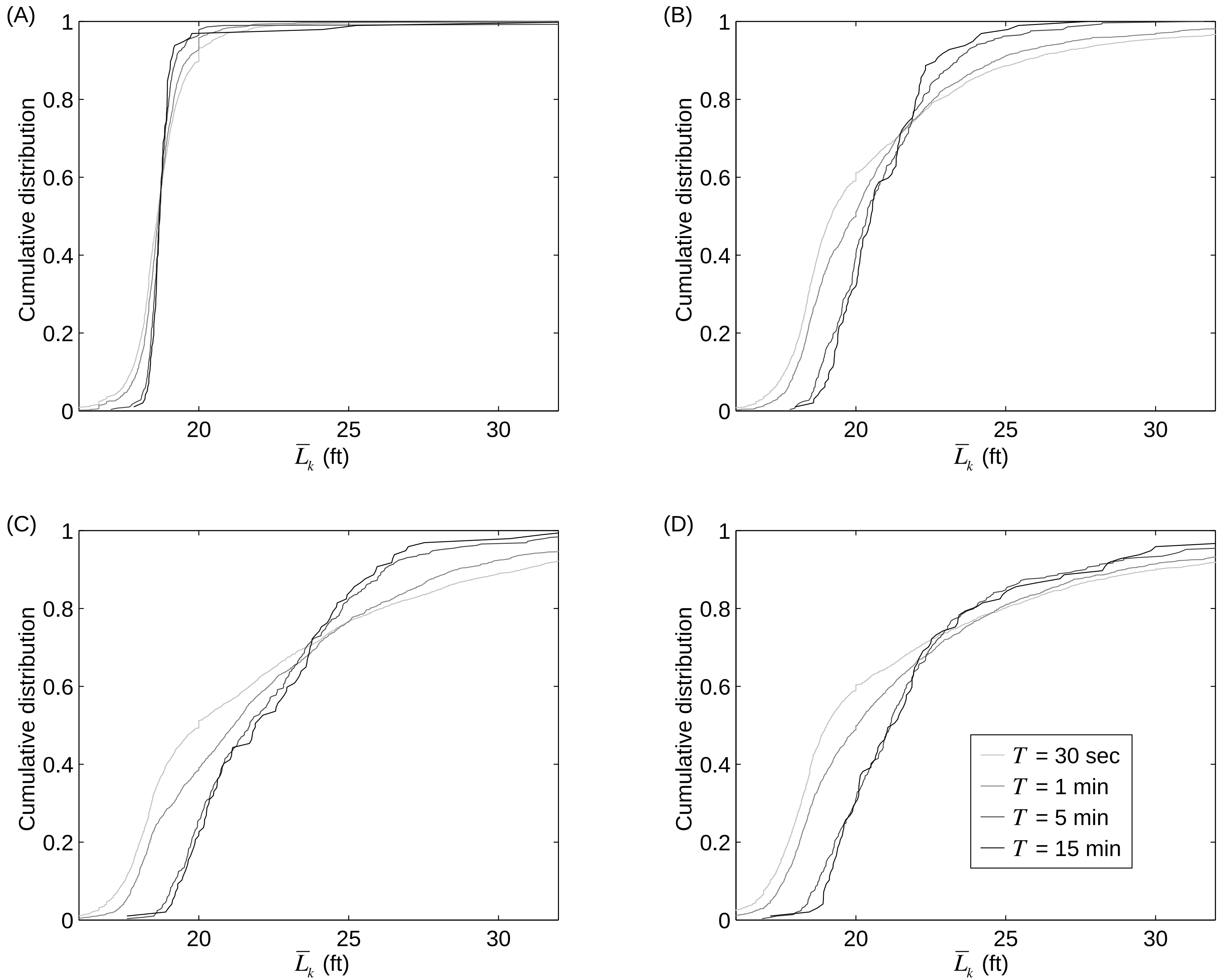

Figure 3, (A) Cumulative distribution of individual vehicle lengths, L_j, for the eastbound lanes, (B) detail of part A.

(A)

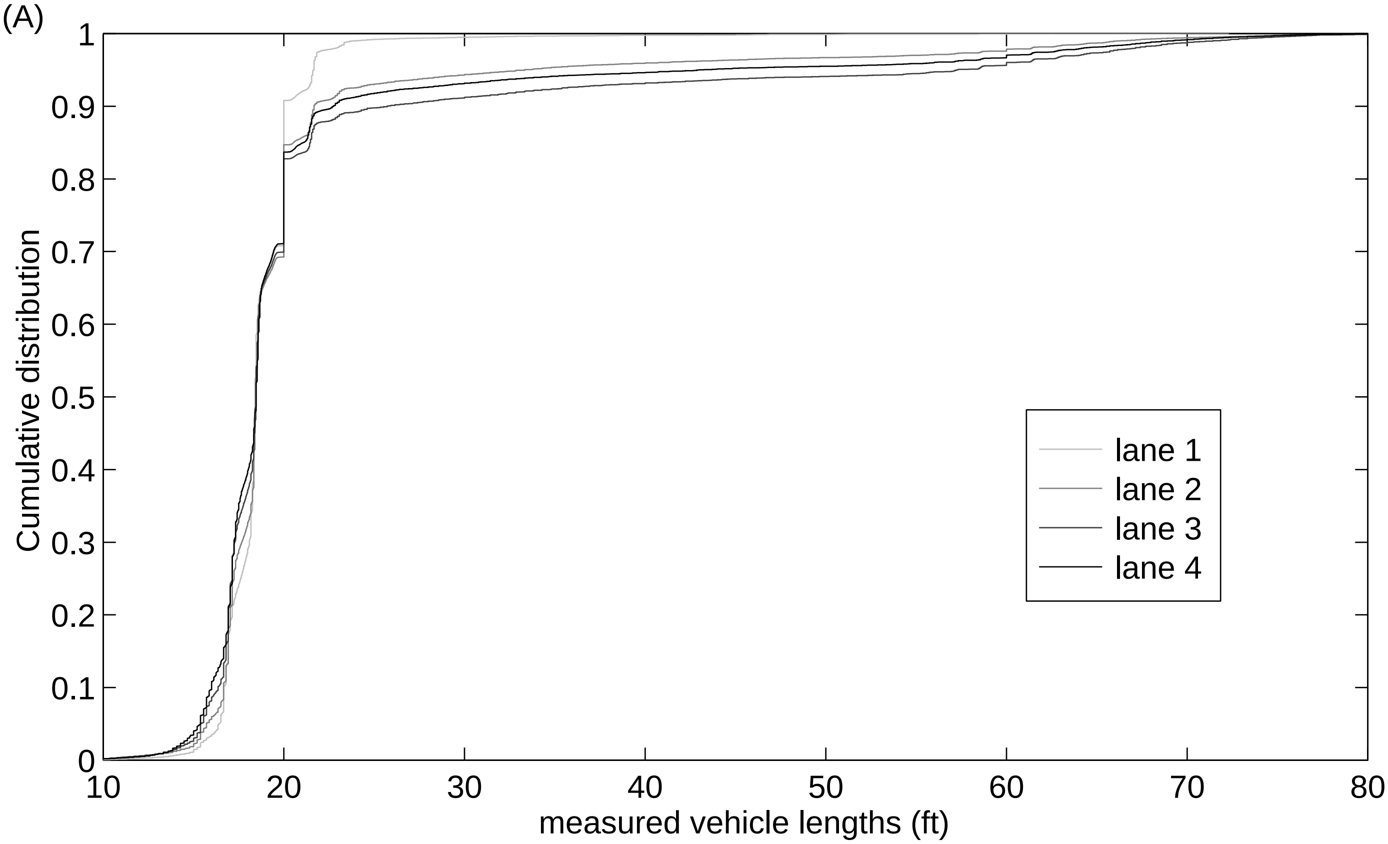

(B)

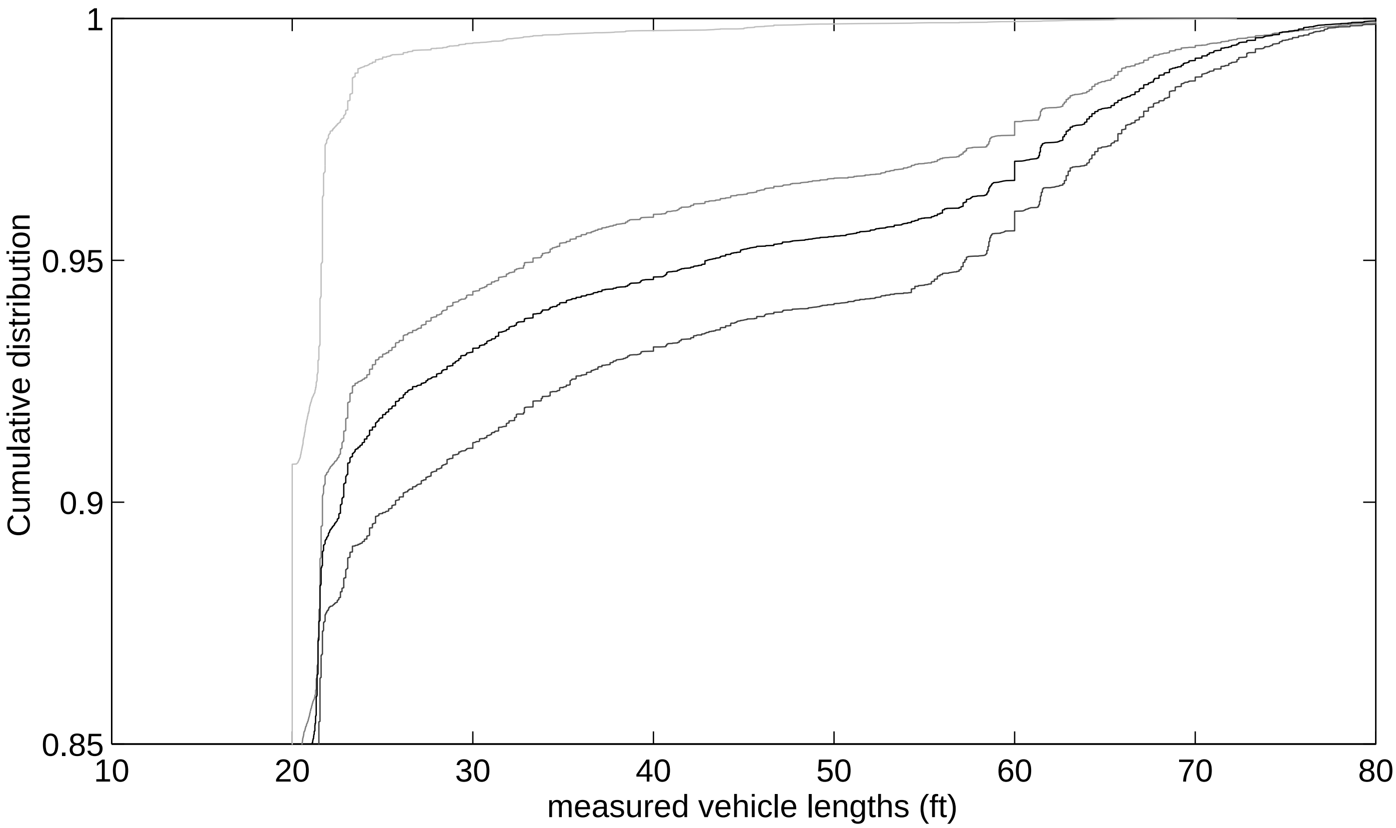

Figure 4, $\bar{L}_k$ versus flow, q_k, for the eastbound traffic: (A)-(C) during free flow, $\bar{v}_k$ > 50 mph and (D)-(F) congestion, $\bar{v}_k$ < 50 mph; sampled at (A) & (D) T = 30 sec, (B) & (E) T = 5 min, (C) & (F) T = 15 min.

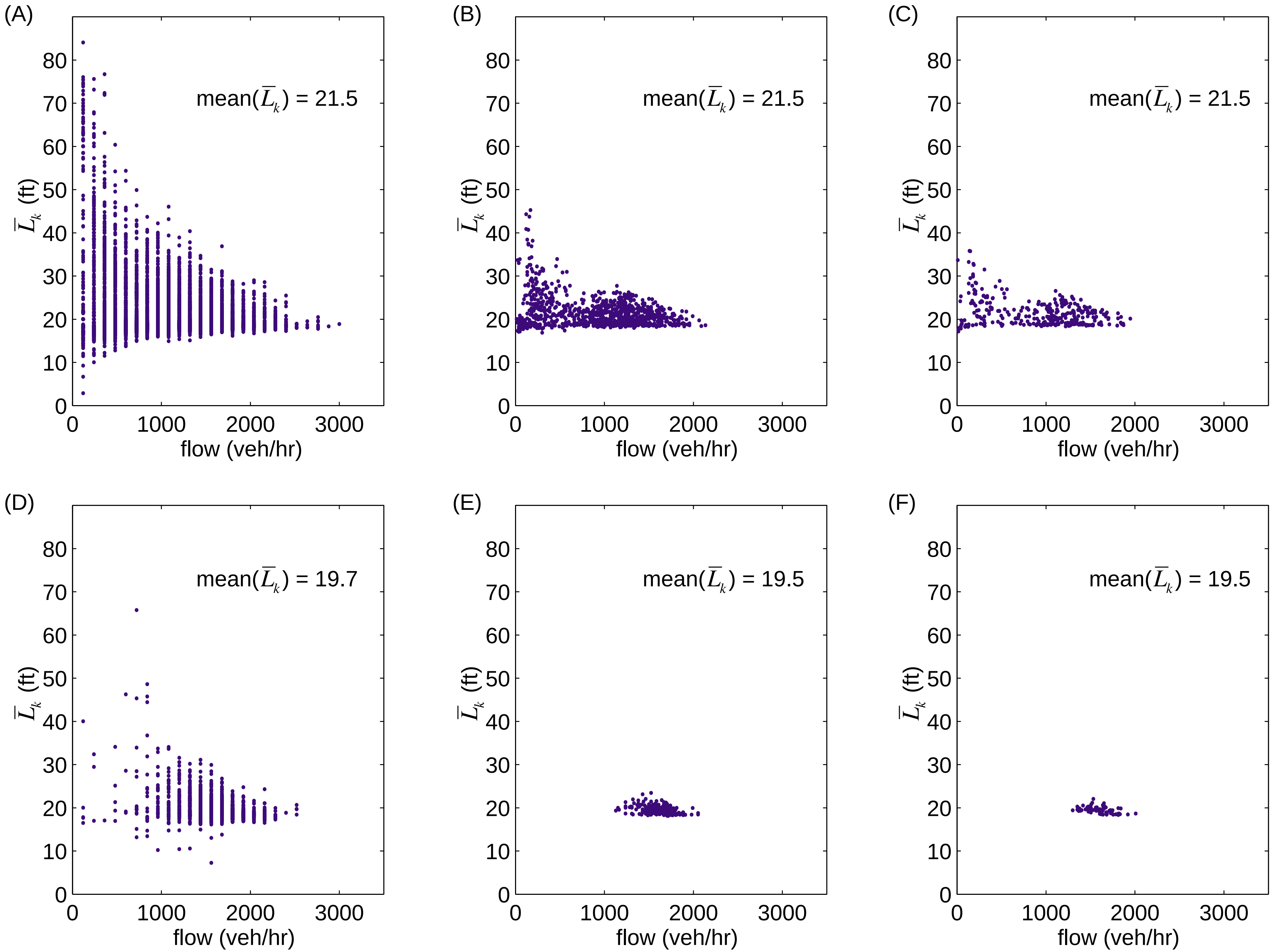

Figure 5, Estimated velocity versus measured velocity, eastbound traffic, T = 30 sec, (A) lane 1, (B) lane 2, (C) lane 3, (D) lane 4.

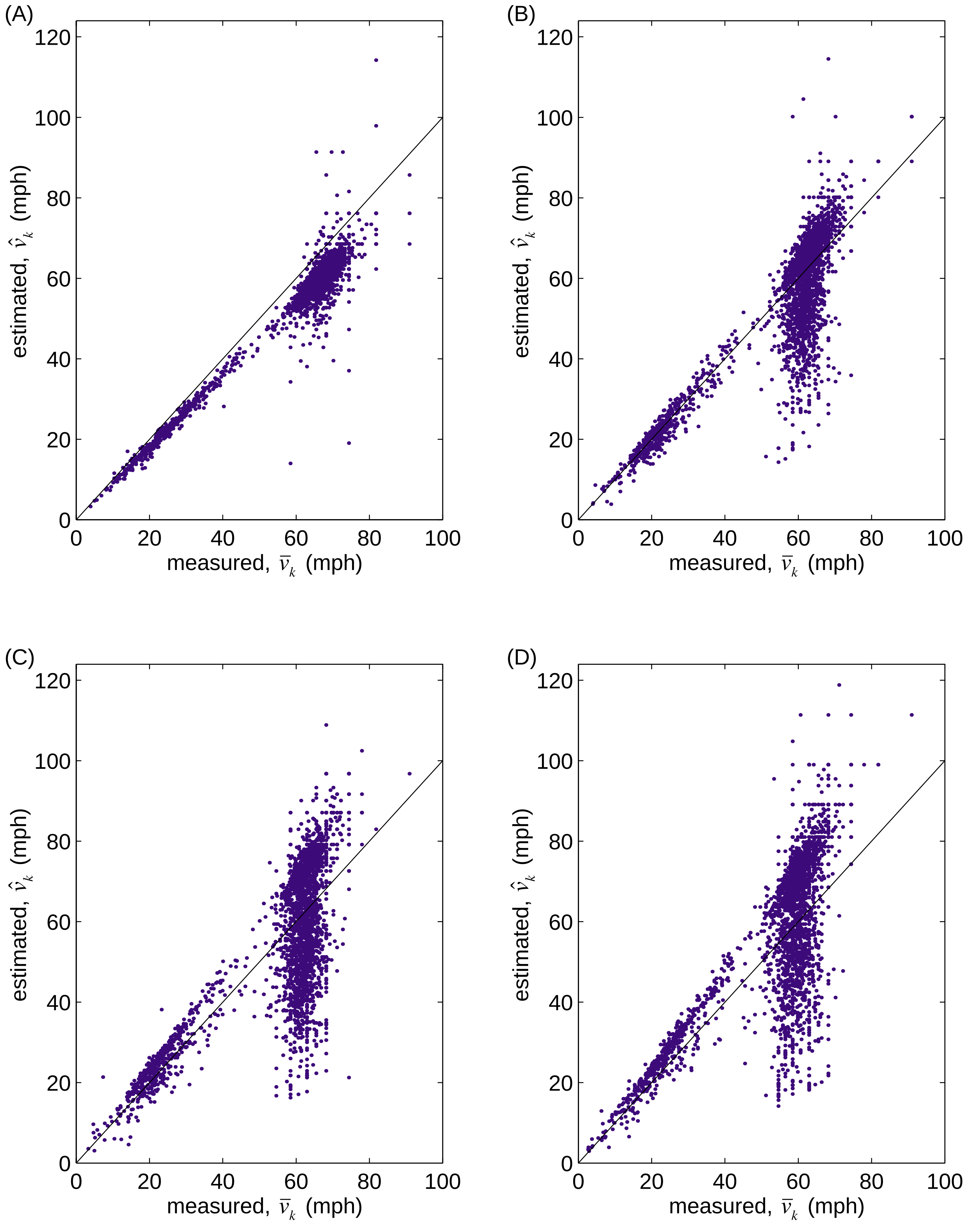

Figure 6, Estimated velocity versus measured velocity, eastbound traffic, T = 5 min, (A) lane 1, (B) lane 2, (C) lane 3, (D) lane 4.

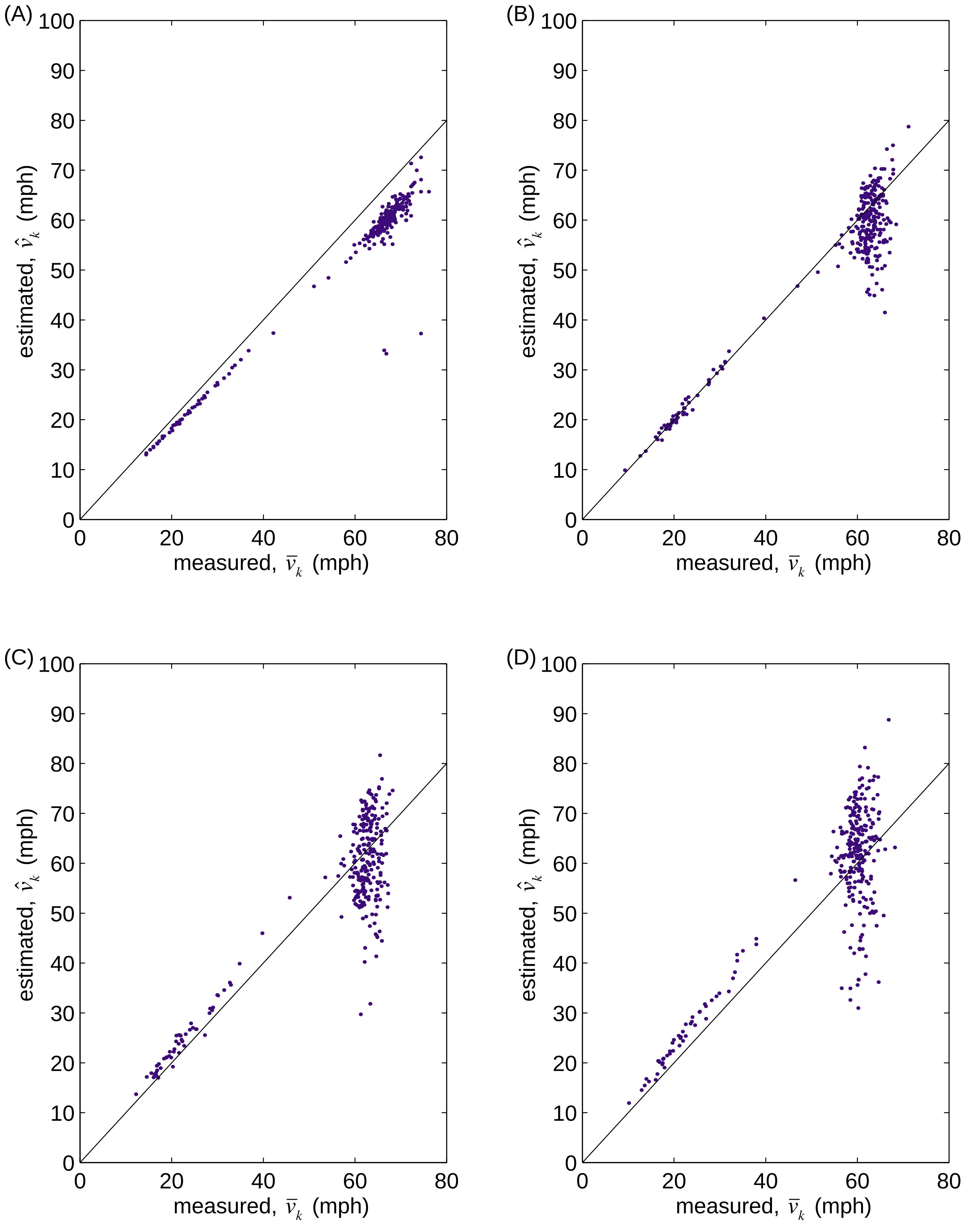

Figure 7, Contour plot showing the cumulative distribution of percent error in estimated velocity as a function of $\hat{L}$, (A)-(B) T = 30 sec, (C)-(D) T = 5 min, for (A) & (C) lane 1 eastbound, (B) & (D) lane 5 westbound.

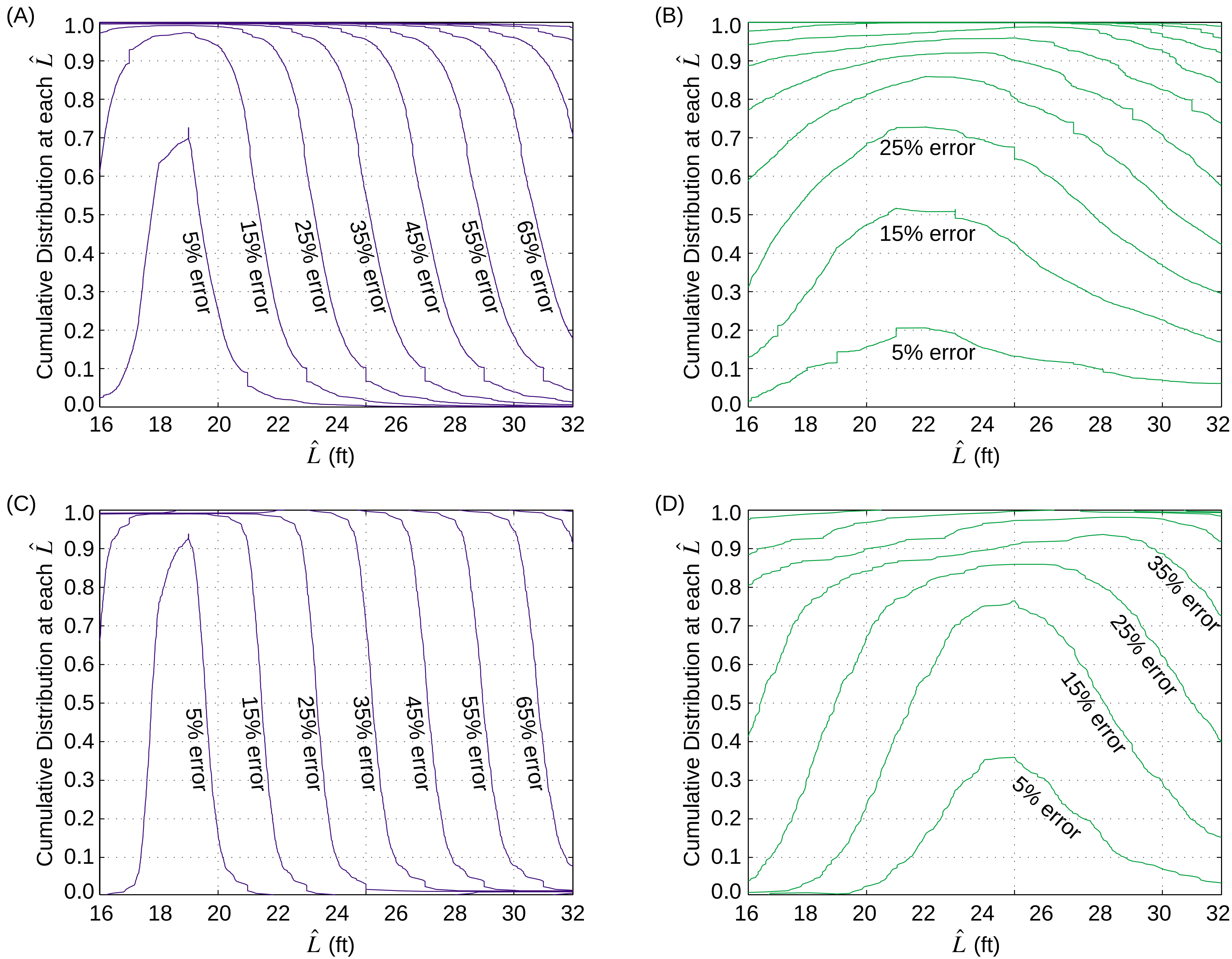

Figure 8, Estimated velocity after identifying low occupancy samples versus measured velocity, eastbound traffic, T = 5 min, (A) lane 1, (B) lane 2, (C) lane 3, (D) lane 4.

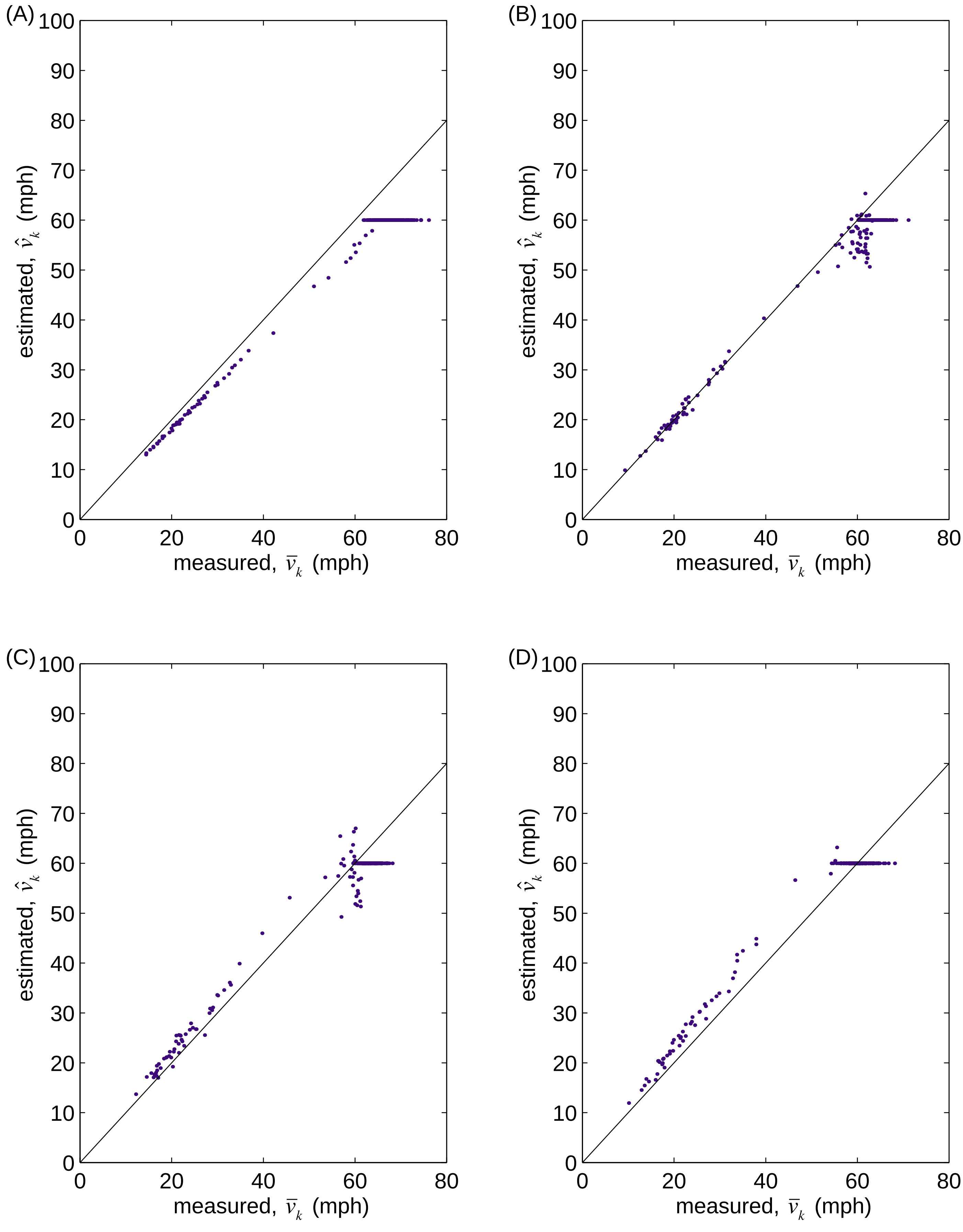

Figure 9, (A) Estimated velocity before identifying low occupancy samples, $\hat{v}_k$, eastbound traffic, T = 5 min and the corresponding (B) estimates after identifying low occupancy samples, (C) measured velocities, $\bar{v}_k$.

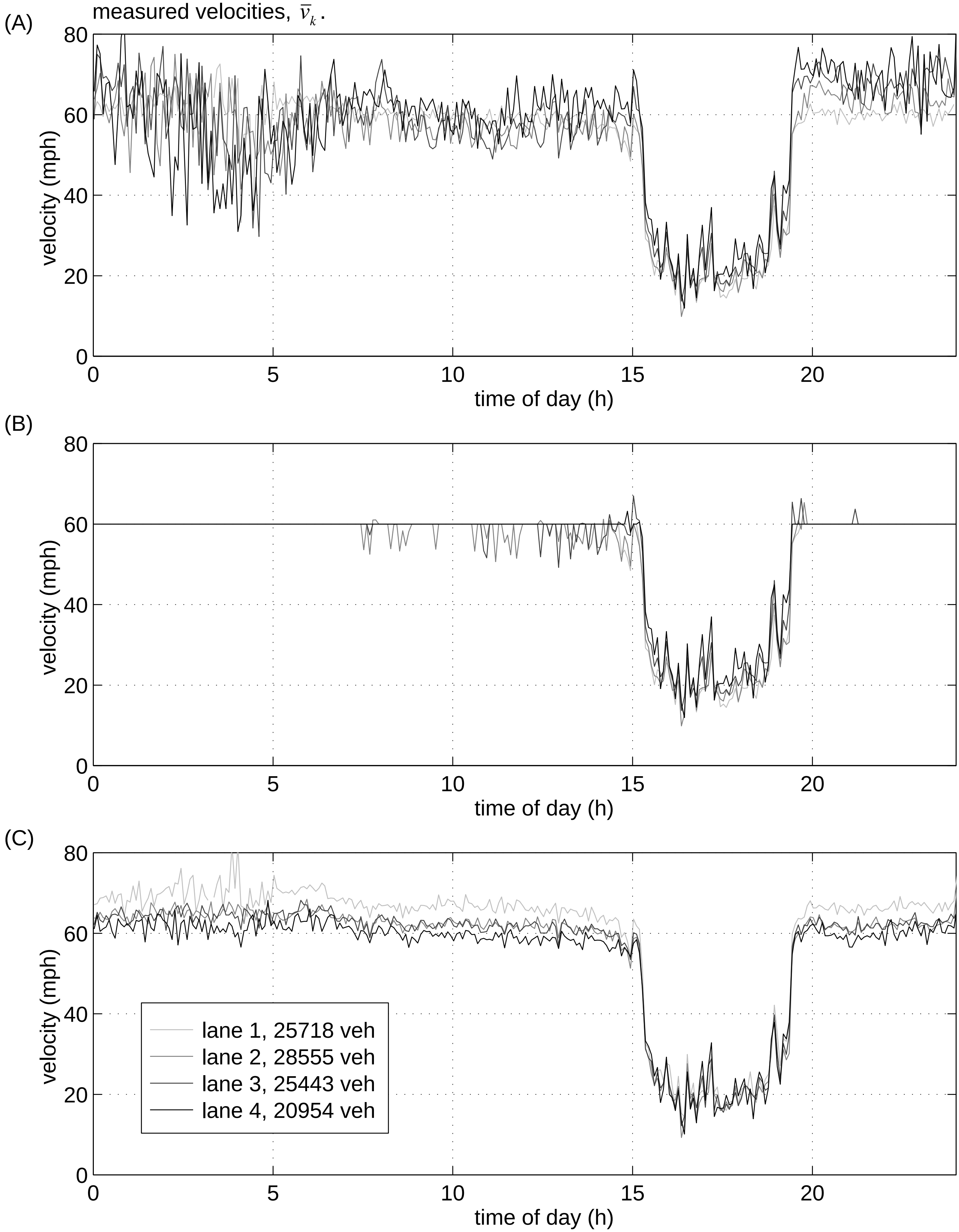

Figure 10, (A) Estimated velocity before identifying low occupancy samples, $\hat{v}_k$, westbound lane 3, T = 30 sec and the corresponding (B) estimates after identifying low occupancy samples, (C) measured velocities, $\bar{v}_k$.

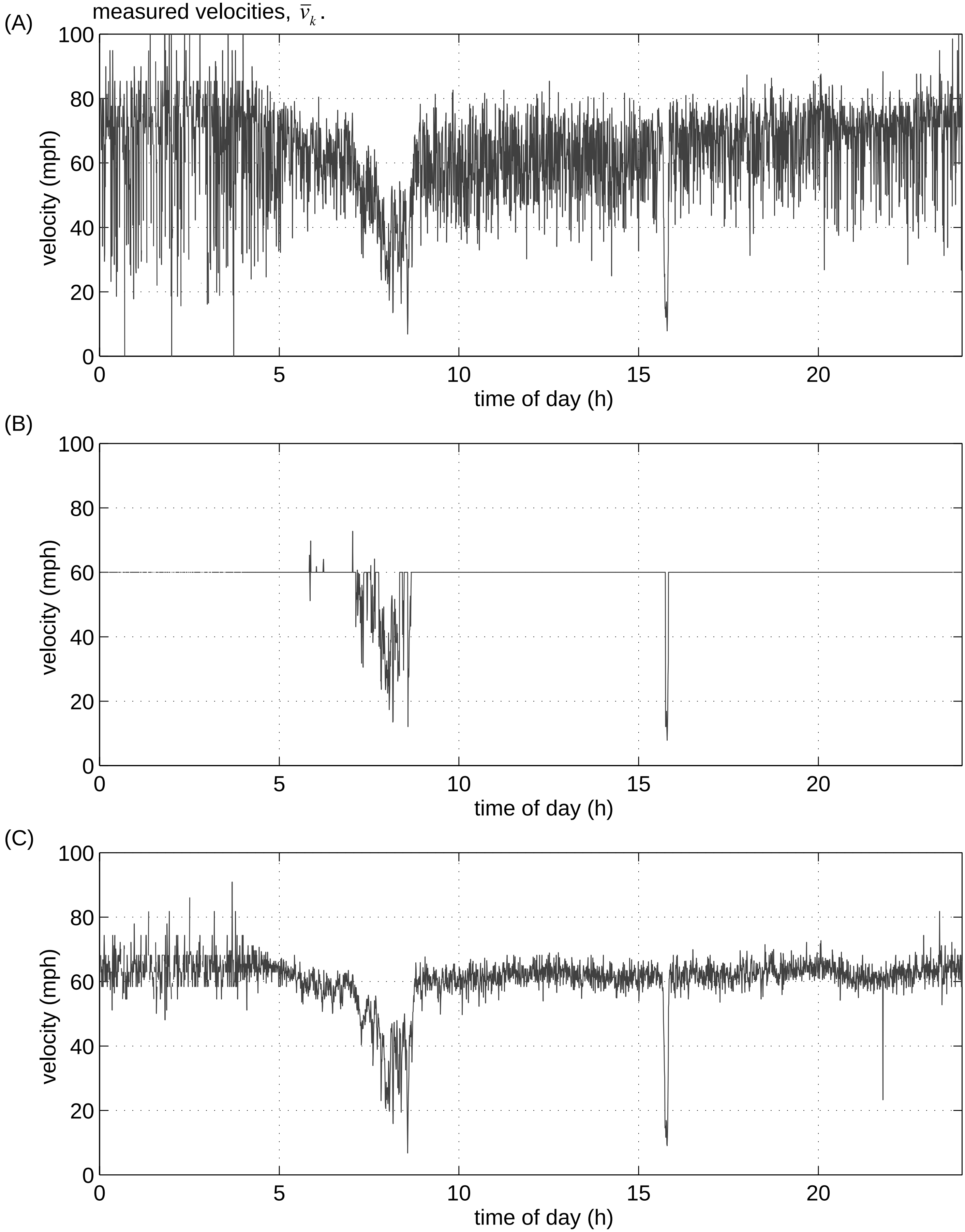

Figure 11, (A) The g-factor versus occupancy, T = 30 seconds, lane 1 eastbound, (B) with occupancy rounded down to integer values, (C) using time mean speed and rounded occupancy.

(A)

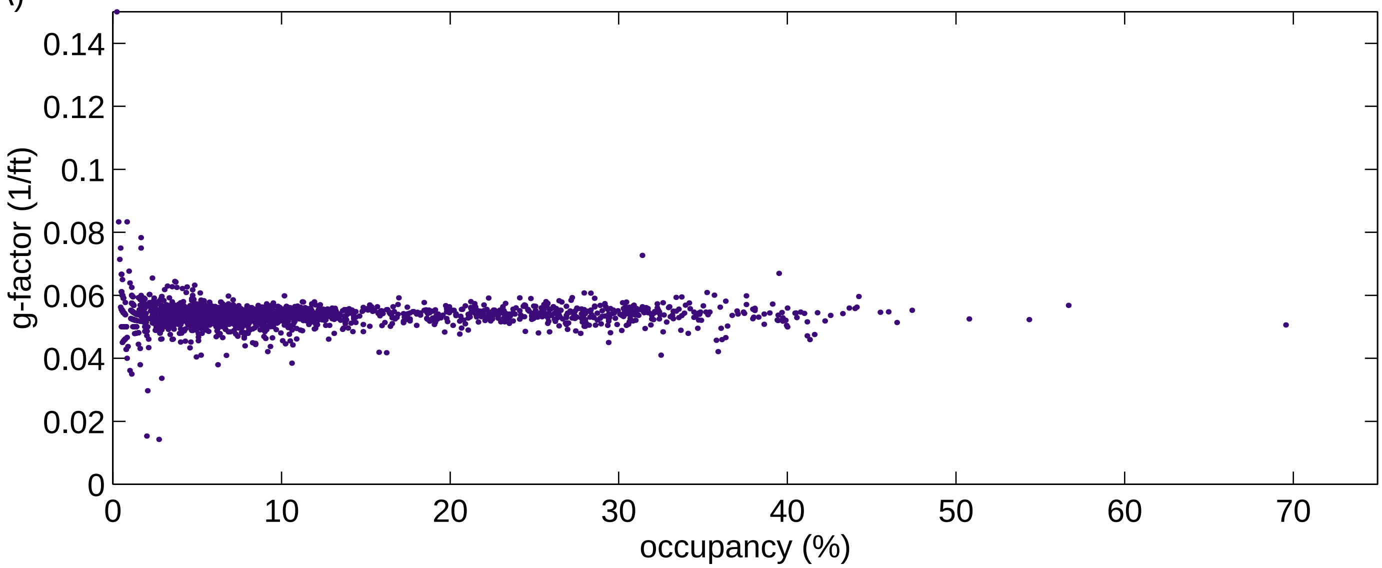

(B)

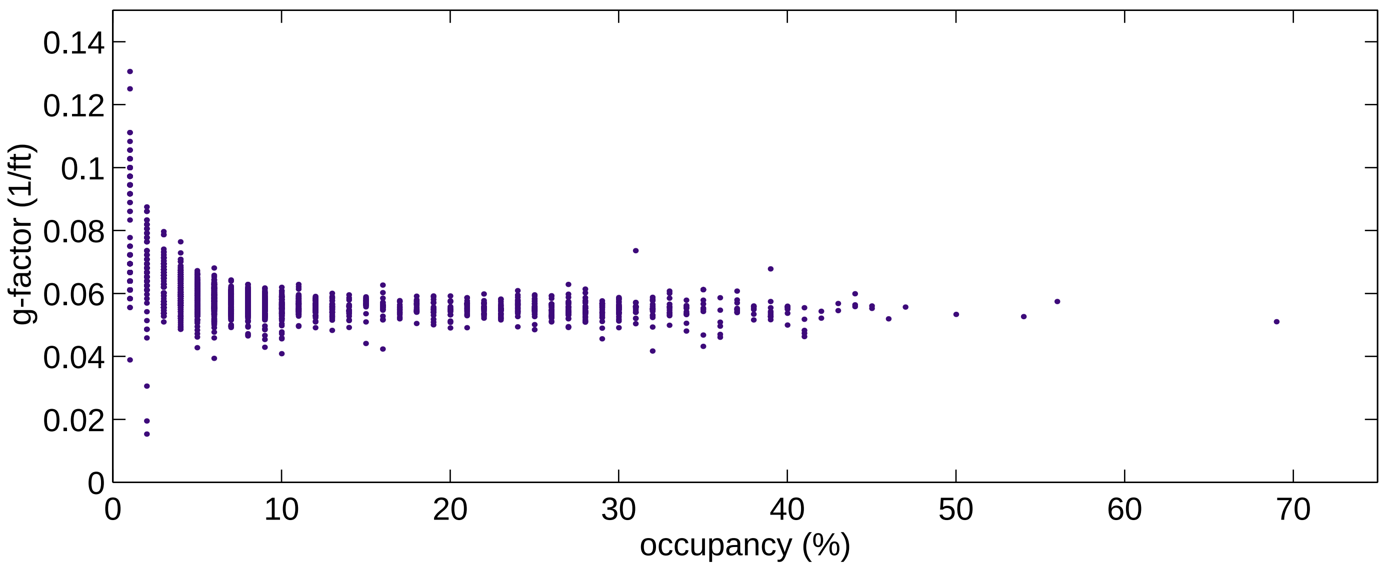

(C)

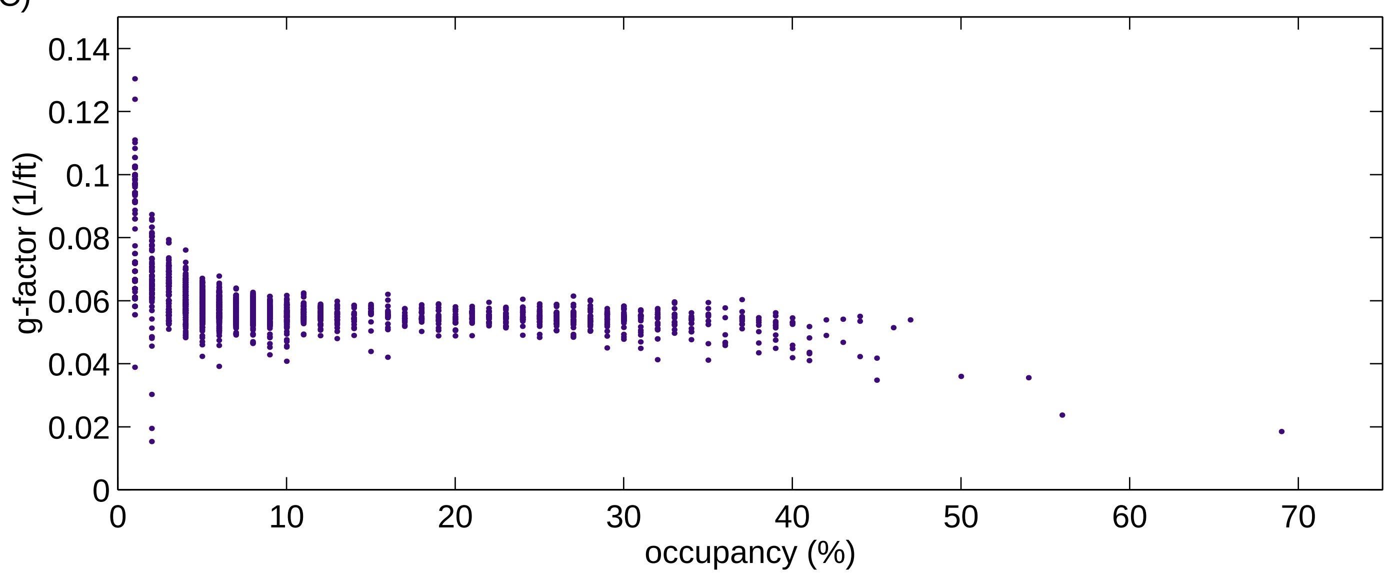

Figure 12, Mean g-factor calculated various ways versus occupancy, T = 30 seconds, for eastbound lane 1. (A) The aggregation method used by Hall and Persaud shown with "X"'s contrasted against the method advocated by this work, (B) the results from two additional aggregation methods.

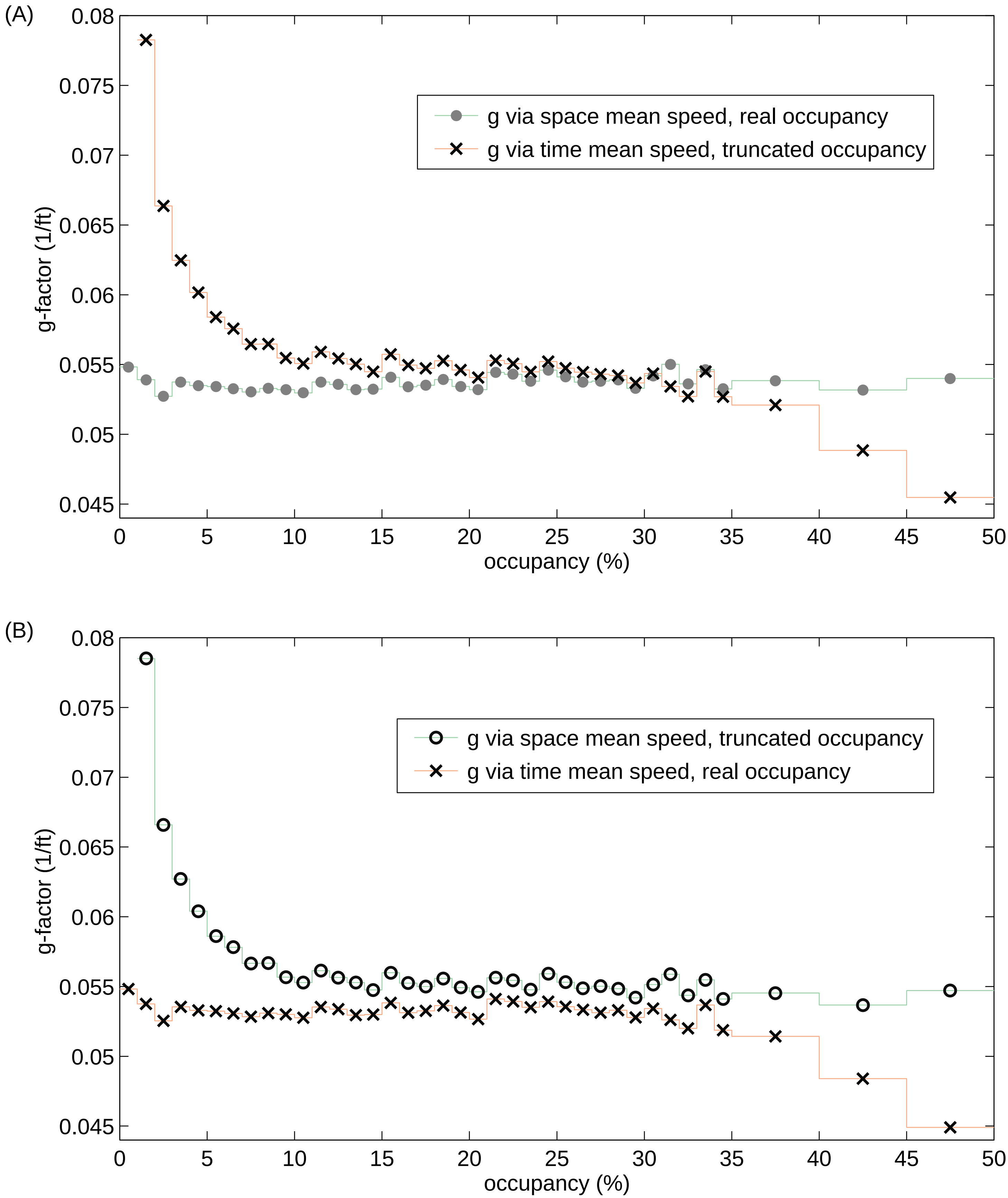

Table 1, The resulting estimates of $\hat{L}$ for the eastbound traffic

Lane	$\hat{L}$ (feet) T = 30 sec	$\hat{L}$ (feet) T = 5 min
1	16.8	16.9
2	19.6	19.9
3	21.3	22.0
4	21.8	22.8